EUKARYOTIC CELL, Dec. 2004, p. 1445–1453 Vol. 3, No. 6
1535-9778/04/$08.00+0 DOI: 10.1128/EC.3.6.1445–1453.2004

Selection and Characterization of RNA Interference-Deficient Trypanosomes Impaired in Target mRNA Degradation

Huafang Shi,[1] Nathalie Chamond,[1] Christian Tschudi,[1,2] and Elisabetta Ullu[1,3]*

Departments of Internal Medicine,[1] Cell Biology,[3] and Epidemiology and Public Health,[2] Yale Medical School, New Haven, Connecticut

Received 20 July 2004/Accepted 2 September 2004

Genetic analysis of the RNA interference (RNAi) pathway in *Trypanosoma brucei* has so far revealed one essential component, namely, *TbAGO1*, encoding a member of the Argonaute protein family. To gain further insight into the RNAi mechanism and its biological significance, we selected RNAi-deficient trypanosomes by using repeated cycles of electroporation with α-tubulin double-stranded RNA, a treatment that blocks cytokinesis in wild-type cells. Two independent clones, termed RiD-1 (for RNAi-deficient clone 1) and RiD-2, were characterized. At the cellular level, only RiD-1 trypanosomes showed a significant increase in doubling time with the concomitant accumulation of cells defective in the completion of cytokinesis. At the RNA level, both clones accumulated wild-type amounts of small interfering RNAs and displayed elevated levels of retroposon transcripts, the hallmark of RNAi deficiency in *T. brucei*. Importantly, both RiD-1 and RiD-2 clones were defective in the degradation of target mRNA, suggesting an impairment of the activity of AGO1, the putative RNAi endonuclease. Since in RiD cells the *AGO1* gene was not mutated and was expressed at wild-type levels, we propose that in trypanosomes the cleavage of mRNA by AGO1 is regulated by the interaction with another factor(s).

RNA interference (RNAi) refers to a posttranscriptional gene-silencing mechanism that is triggered in many eukaryotic organisms by double-stranded RNA (dsRNA). Early on it was recognized that one of the biological functions of RNAi is to destroy transcripts derived from molecular parasites, namely, viruses, transposons, retroposons, or transgenes. However, in the course of the last few years it has become evident that the RNAi pathway is also implicated in a variety of gene-silencing phenomena as diverse as heterochromatin assembly (29) and maintenance (9), DNA and histone methylation (32), programmed gene rearrangement in *Tetrahymena* (17), promoter silencing (16), and developmental control (12, 13).

The classical RNAi pathway, triggered by synthetic or transgene-derived dsRNA of up to several hundred nucleotides in length, is best described as a two-step reaction, namely, the initiation and effector steps (10). In the initiation step, dsRNA is processed by Dicer, an RNase III-related enzyme, into 19- to 26-nucleotide (nt)-long small interfering RNAs (siRNAs), which are the hallmark of the RNAi pathway. Subsequently, siRNAs are transferred to the RNAi-silencing complex (RISC), most likely with the assistance of R2D2 (15), a dsRNA binding protein. In the effector step, RISC carries out targeting and degradation of homologous transcripts. Recently, the mammalian Argonaute2, a member of the Argonaute (AGO) family, has been shown to be the RNAi endonuclease or "slicer" that carries out mRNA degradation in RISC (14). Several other proteins are associated with *Drosophila* RISC, namely, VIG (for vasa intronic gene), FXR (for fragile-X-related protein, the *Drosophila* homologue of the human fragile-X mental retardation syndrome protein or FMRP), the helicase p68 (4, 11), and Tudor-SN, a protein containing five staphylococcal/micrococcal nuclease-like domains and a Tudor domain (3). Furthermore, the *Drosophila* helicase armitage has been recently shown to be required in the early steps of RISC assembly (23). At present, with the exception of mammalian AGO2 (14), the specific functions of the other RISC-associated proteins are not understood.

From an evolutionary point of view, the RNAi pathway was an early acquisition of eukaryotes, as RNAi is functional in *Trypanosoma brucei*, a parasitic protozoon that is considered an early divergent eukaryote. Since its discovery in 1998 (19), RNAi has become the method of choice to study gene function in trypanosomes and has provided a tool for forward genetic approaches (30), as well as for global analysis of gene function. At the mechanistic level, dsRNA derived from synthetic dsRNA, from transgenes, or from retroposons (5, 6) is diced to siRNAs by a putative Dicer, whose identity is at present unknown. siRNAs are in a complex with TbAGO1, a member of the Argonaute protein family, which is at present the only known component of RISC in *T. brucei* (21). Current evidence from our laboratory is consistent with TbAGO1 being the RNAi endonuclease in *T. brucei* (21a). The AGO1-siRNA ribonucleoprotein complex is found both in a soluble form and associated with translating ribosomes. We have proposed that the association between the AGO1-siRNP complex and polyribosomes facilitates recognition and destruction of target mRNA by RISC while the mRNA is being translated or marks the mRNA for subsequent degradation in the cytoplasm (25).

Genetic ablation of *TbAGO1* completely disables the RNAi pathway: the accumulation of transgene- or retroposon-derived siRNAs is drastically reduced, most likely because association with AGO1 is required to stabilize siRNAs, and target mRNAs are not degraded (21). These studies also showed that

* Corresponding author. Mailing address: Department of Internal Medicine, Yale Medical School, BCMM 136D, 295 Congress Ave., Box 9812, New Haven, CT 06536-8012. Phone: (203) 785-3563. Fax: (203) 785-7329. E-mail: elisabetta.ullu@yale.edu.

TbAGO1 controls the abundance of retroposon transcripts by a mechanism operating at the levels of transcription and RNA stability. Thus, like in plants and C*aenorhabditis elegans*, RNAi in *T. brucei* functions as a genome defense mechanism to silence retroposon transcripts. Furthermore, it has recently been reported that genetic ablation of *TbAGO1* in a derivative of *T. brucei* 427 results in severe defects in mitosis and in aberrant chromosome segregation (7). Interestingly, these phenotypes are reminiscent of those described for certain RNAi mutants of *Schizosaccharomyces pombe* (2, 8, 28) and point to a potential role of *TbAGO1* in centromeric heterochromatin assembly.

As an independent means to further our understanding of the mechanism and biological significance of RNAi in trypanosomes, we developed a selection procedure to derive cell lines that are defective in the RNAi pathway. Acquisition of this trait does not require mutagenesis prior to selection nor is it dependent on whether uncloned or freshly cloned lines are used as starting populations for selection, and it can occur in different trypanosome strains. Analysis of two independently selected clones provides evidence that, in both instances, RNAi deficiency resulted from impairment in the last step of the RNAi pathway.

MATERIALS AND METHODS

Growth and manipulation of cells. YTat 1.1 procyclics were maintained at 27°C as previously described (21). Selection of cells resistant to α-tubulin dsRNA challenge was performed as follows. Trypanosomes (10^9) were divided in 10 aliquots, and each aliquot was electroporated with 10 μg of synthetic α-tubulin dsRNA corresponding to the 5′ untranslated region of α-tubulin mRNA as previously described (19) and then returned to culture for expression of the FAT phenotype. After approximately 48 h of growth, the cells in the medium were removed from the culture, taking care not to disturb the cells at the bottom of the flask, which consisted mainly of large aggregates of FAT cells. The surviving cells were collected by centrifugation, resuspended in 10 ml of fresh medium, and allowed to grow until they reached a cell density of about 10^7/ml. At this point a second round of electroporation and growth was performed, and this procedure was repeated a total of five times. Clonal RiD-1 and RiD-2 cell lines were then established by limited dilution in microtiter dishes.

Nucleic acid and protein analyses. Northern and Western blot analyses were performed as previously described (21). For expression of green fluorescent protein (GFP) dsRNA, cells were transformed with a plasmid construct expressing hairpin GFP dsRNA as previously described (21). Synthesis of radiolabeled RNA in permeable cells was carried out as previously described (24).

Cytological and immunofluorescence assays. For determination of the cell cycle status, trypanosomes were spread onto microscope slides and air dried. The slides were fixed for at least 30 min in 100% methanol at −20°C and stained with DAPI (4,6-diamidino-2-phenylindole). At least 500 cells were counted for each cell line, and three independent cell counts were carried out on different, independently grown cell populations. The flagellum was stained with a monoclonal mouse antibody directed to the paraflagellar rod protein (PFR) (19), followed by 1 μg of Alexa Fluor 586-conjugated goat anti-mouse antibody [goat anti-mouse immunoglobulin G (heavy plus light chain) $F(ab')_2$ fragment conjugate from Molecular Probes] per ml.

FACS analysis. Cells were resuspended at a density of 2×10^6/ml in 70% ice-cold ethanol and fixed overnight at 4°C. The cell pellet was resuspended in phosphate-buffered saline containing 1 mg of glucose per ml, 10 μg of propidium iodide per ml, and 10 μg of RNase A per ml and incubated at room temperature for 30 min. Fluorescence-activated cell sorting (FACS) was performed with a Becton Dickinson FACSCalibur with detector FL2-A and an AmpGain of 1.85. Data were analyzed by using the software CellQuest version 3.3.

RESULTS

Selection and characterization of trypanosomes resistant to challenge with α-tubulin dsRNA. One of the properties of electroporation of synthetic dsRNA in *T. brucei* is its high efficiency, which routinely approaches 90 to 98%. In particular, we have previously shown that transfection of trypanosomes with α-tubulin dsRNA results in degradation of target mRNA and transient downregulation of α-tubulin synthesis (19). At the cellular level cytokinesis is blocked, but the cells continue to duplicate various organelles, lose cytoskeleton integrity, and increase in volume (FAT phenotype). FAT cells form large aggregates and eventually die. This observation provided a powerful and simple approach to enrich for trypanosomes that are defective in the acquisition of the FAT phenotype (Fig. 1). We reasoned that among the cells unable to become FAT in response to electroporation of α-tubulin dsRNA, we might recover trypanosomes that were defective at some step of the RNAi pathway. In a pilot experiment, 10^9 insect-form (procyclic) *T. brucei rhodesiense* YTat1.1 cells, without prior mutagenesis, were electroporated with saturating amounts of α-tubulin dsRNA and allowed to grow in order to develop the FAT phenotype. Next, the cells that had not acquired the FAT phenotype, which represented 2 to 5% of the initial cell population, were separated from FAT cells and expanded (see Materials and Methods for details). This constituted one selection cycle. We performed five successive rounds of electroporation and growth, and after the fifth round more than 90% of the cells did not acquire the FAT phenotype upon challenge with α-tubulin dsRNA. To exclude the possibility that the α-tubulin dsRNA-resistant cells had become resistant to taking up nucleic acids by electroporation, we measured the efficiency of transient expression of a plasmid expressing GFP. The result of this test showed no significant difference in transfection efficiency between wild-type and α-tubulin dsRNA-resistant cells (data not shown). Next, we transfected into the α-tubulin dsRNA-resistant cells a plasmid engineered for high levels of expression of α-tubulin dsRNA as a hairpin (19). Even when the dsRNA was produced inside the cells, the α-tubulin dsRNA-resistant cells did not acquire the FAT phenotype (data not shown). This test eliminated the possibility of defects in the uptake of dsRNA. On the basis of these observations we concluded that the α-tubulin dsRNA-resistant cells were likely to be impaired in responding to α-tubulin dsRNA, possibly because they were defective at some step of RNAi. Northern blot analysis of the fate of α-tubulin or actin mRNA following

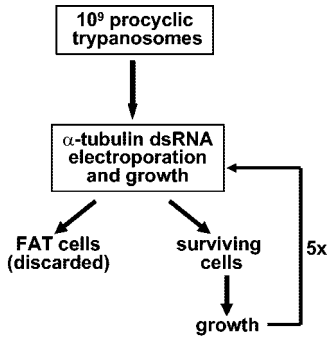

FIG. 1. Selection of trypanosomes resistant to killing by electroporated α-tubulin dsRNA. A schematic representation of the selection regimen used to enrich for α-tubulin dsRNA-resistant trypanosomes is shown. See text for details.

transfection of the corresponding dsRNA confirmed this possibility (data not shown, but see Fig. 4).

Having established a proof of principle, we decided to test whether the genetic background of the starting trypanosome population affected the selection process. Indeed, our laboratory strain, YTat1.1, had been propagated in culture for several years, and it was likely that its genetic constitution was heterogeneous. Thus, we derived two clonal cell lines, termed Y1 and Y2, from the YTat1.1 trypanosome population and subjected each of them to the selection procedure described above. As observed before, after five cycles of electroporation and growth more than 90% of the cells failed to respond to challenge with α-tubulin dsRNA. Next, to test whether acquisition of resistance to α-tubulin dsRNA was a specific property of our *T. brucei* laboratory strain, the same selection procedure was applied to two other *T. brucei* laboratory strains. These were 29.13 procyclics (a derivative of *T. brucei* 427), which are commonly used for establishing tetracycline-inducible expression (31), and *T. brucei brucei* 927 procyclics, the trypanosome strain used for genome sequencing (26). In both cases, cells resistant to α-tubulin dsRNA could be obtained (data not shown). However, it required seven to eight selection cycles for the 29.13 and 927 trypanosomes to become more than 90% resistant to α-tubulin dsRNA, compared to five cycles as we observed with the uncloned YTat 1.1 strain or the clonal derivatives Y1 and Y2.

The α-tubulin dsRNA-resistant trypanosomes derived from selection of the Y1 and Y2 cell lines were then cloned by limited dilution. One clone from each of the two populations, namely, Y1-13 and Y2-11, were selected as being representative of several that showed the least response to α-tubulin dsRNA. Henceforth these clones will be referred to as RiD-1 (for RNAi-deficient clone 1) and RiD-2.

Cell cycle and cytological analysis of RiD trypanosomes. During the course of our analyses, we observed that RiD-1 trypanosomes were growing more slowly than wild-type and RiD-2 trypanosomes. To precisely determine the extent of the growth defect, we monitored cell growth rates in the following way. Cells were seeded at 5×10^5/ml, allowed to grow for 24 h, counted, and diluted again to 5×10^5/ml. This procedure was repeated six times. Figure 2A shows the average number of cells per milliliter after a 24-h period of growth, and from these results we calculated the average doubling time (Fig. 2B) for each cell line. Compared to that of wild-type Y2 cells, the doubling time of RiD-2 cells was slightly increased (8.8 versus 8.3 h), whereas the doubling time of RiD-1 cells was 10.9 h. This corresponds to about a 30% increase in the duration of cell cycle and is similar to the growth rate defect of our previously established *ago1*$^{-/-}$ cells (21). Cells in which the *AGO1* deletion was complemented by reintroducing one copy of the *AGO1* gene at its chromosomal location (*ago1c*) had only a slight growth defect (8.5 versus 8.3 h) compared to wild-type cells.

In order to identify the potential cell cycle defect(s) underlying the increase in cell cycle length in RiD-1 and *ago1*$^{-/-}$ cells, we labeled DNA with propidium iodide and analyzed the DNA contents of the various cell populations by FACS analysis. As shown in Table 1, wild-type, RiD-1, RiD-2, *ago1*$^{-/-}$, and *ago1c* trypanosomes had similar distributions of cells with DNA contents corresponding to 2C (cells in G_1), 4C (cells in G_2 plus postmitotic cells), or between 2C and 4C (cells in S phase). However, both *ago1*$^{-/-}$ and RiD-1 cells showed approximately a 1.5- to 2-fold increase in the proportion of cells with a DNA content greater than 4C. In contrast, among the five cell lines we analyzed we could not detect any statistically

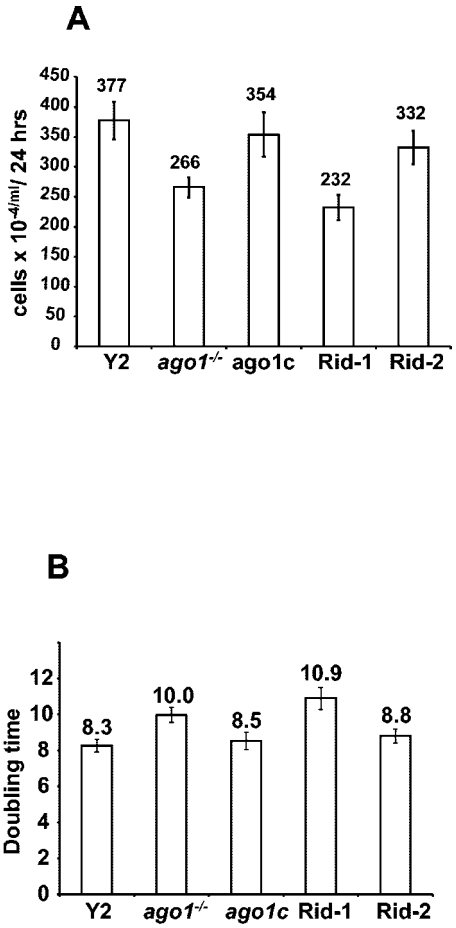

FIG. 2. (A) Growth characteristics of wild-type (Y2), RNAi-deficient (RiD-1 and RiD-2), *ago1*$^{-/-}$, and *ago1c* (*ago*$^{-/-}$ cells complemented with one allele of *AGO1*) cells. Cells were counted and diluted to 5×10^5/ml every 24 h for six consecutive cycles. The average number of cells after a 24-h period of growth is shown for each cell line. (B) The doubling time of each cell line was calculated from the data shown in panel A by using the equation $x\log 2 = \log(y/5)$, where x is the number of generations and y is the number of cells times 10^5/ml as determined 24 h after seeding; $24/x$ is the doubling time. Error bars indicate standard deviations.

TABLE 1. DNA contents of wild-type (Y2), RNAi-deficient (RiD-1 and RiD-2), *ago1*$^{-/-}$, and *ago1c* cells as determined by FACS analysis

Cell type	% DNA content (mean ± SD)				
	<2C	2C	>2C and <4C	4C	>4C
Y2	1.1 ± 0.22	45.3 ± 2.76	19.9 ± 1.01	30.9 ± 2.93	3.3 ± 0.37
ago1$^{-/-}$	1.6 ± 0.50	42.5 ± 1.28	19.7 ± 1.95	30.6 ± 2.18	6.3 ± 0.90
ago1c	0.4 ± 0.04	48.0 ± 2.47	20.3 ± 1.29	29.2 ± 2.40	2.5 ± 0.19
RiD-1	1.2 ± 0.42	48.9 ± 3.56	18.9 ± 1.17	26.1 ± 3.02	5.3 ± 0.35
RiD-2	1.0 ± 0.17	46.7 ± 4.30	20.2 ± 1.48	29.1 ± 3.34	3.5 ± 0.24

TABLE 2. Analysis of the cell cycle status of wild-type (Y2), RNAi-deficient (RiD-1 and RiD-2), *ago1*$^{-/-}$, and *ago1c* cells

Cell type	% Cell type (mean ± SD)				
	1K1N	2K1N	2K2N	1K0N	4K2-4N
Y2	84.2 ± 2.56	6.0 ± 2.21	5.3 ± 2.53	0.88 ± 0.48	0 ± 0
ago1$^{-/-}$	77.3 ± 3.49	9.5 ± 2.30	6.9 ± 2.14	1.90 ± 0.62	1.69 ± 1.27
ago1c	79.4 ± 0.92	9.7 ± 1.32	8.5 ± 1.59	0.90 ± 0.50	0.39 ± 0.16
RiD-1	78.0 ± 1.83	9.8 ± 1.34	6.8 ± 1.29	1.88 ± 1.16	1.78 ± 0.68
RiD-2	81.8 ± 1.89	7.2 ± 1.77	6.8 ± 2.75	0.46 ± 0.24	0.42 ± 0.60

significant difference in the percentage of cells with a DNA content less than 2C. Cells in this category would include zoids (20), namely, cytoplasmic fragments containing kinetoplast (mitochondrial) DNA but devoid of nuclei.

Next, the cell cycle statuses of the various cell populations were monitored by using DAPI staining to visualize the nucleus and kinetoplast in each cell. The cell cycle position of trypanosomes can be readily defined by the nucleus and kinetoplast number in individual cells: G_1 and S-phase cells have one kinetoplast and one nucleus (1K1N), G_2 cells have two kinetoplasts and one nucleus (2K1N), and postmitotic cells have two kinetoplasts and two nuclei (2K2N). Relative to wild-type cells, RiD-1, RiD-2, *ago1*$^{-/-}$, and *ago1c* trypanosomes showed a small decrease in the percentage of 1K1N cells and a concomitant small increase in 2K1N cells (Table 2). Furthermore, *ago1*$^{-/-}$ and RiD-1 cells displayed a slight increase in the number of zoids (1K0N) but a more pronounced increase in a novel type of cells with two to four nuclei and at least four kinetoplasts (4K2-4N). Figure 3 shows some examples of the morphology of these aberrant trypanosome cells, which we termed "stuck" cells. Stuck cells consist of two trypanosomes still connected at the posterior end, as is typical of cells at the last stages of cytokinesis, but these cells had initiated a new cell cycle, as evidenced by the number of kinetoplasts and flagella, and in some instances had completed a second round of mitosis (cells with more than two nuclei). Thus, stuck cells were derived from trypanosomes that had not completed cytokinesis at the previous cell cycle.

RiD-1 and RiD-2 trypanosomes are defective in degradation of target mRNA but accumulate wild-type levels of siRNAs. To define which step in the RNAi pathway was affected in RiD trypanosomes, we monitored the extent of degradation of target mRNA upon electroporation of wild-type (Y2), RiD-1, and RiD-2 cells with increasing doses of each of two different dsRNA triggers, namely, α-tubulin and PFR dsRNAs. Total RNA for Northern blot analysis was isolated 2 h after transfection, as mRNA degradation is maximal at 1 to 2 h after transfection with dsRNA (19). In addition, a sample of each cell culture was grown for 16 h to allow expression of the FAT phenotype. Although RNAi downregulation of PFR expression results in defects in the assembly of the paraflagellar rod in the new flagellum (1), we did not analyze this phenotype in this study. Figure 4 shows that, with 1, 2, or 5 μg of α-tubulin dsRNA, wild-type cells gave rise to 57, 81, or 92% FAT cells, respectively. In contrast, under the same conditions, RiD-1 and RiD-2 clones showed a dramatic impairment in their ability to respond to α-tubulin dsRNA challenge. In particular, at concentrations of dsRNA below saturation, namely, 1 and 2 μg/transfection, both clones showed either undetectable amounts of FAT cells or about 0.5 or 1.0% FAT cells, respectively. However, at 5 μg of α-tubulin dsRNA/transfection, RiD-1 and RiD-2 clones gave rise to about 5 and 7% FAT cells, respectively. These results were consistent with the interpretation that RiD-1 and RiD-2 represented cell lines that have a severe impairment to challenge by α-tubulin dsRNA, but retain the

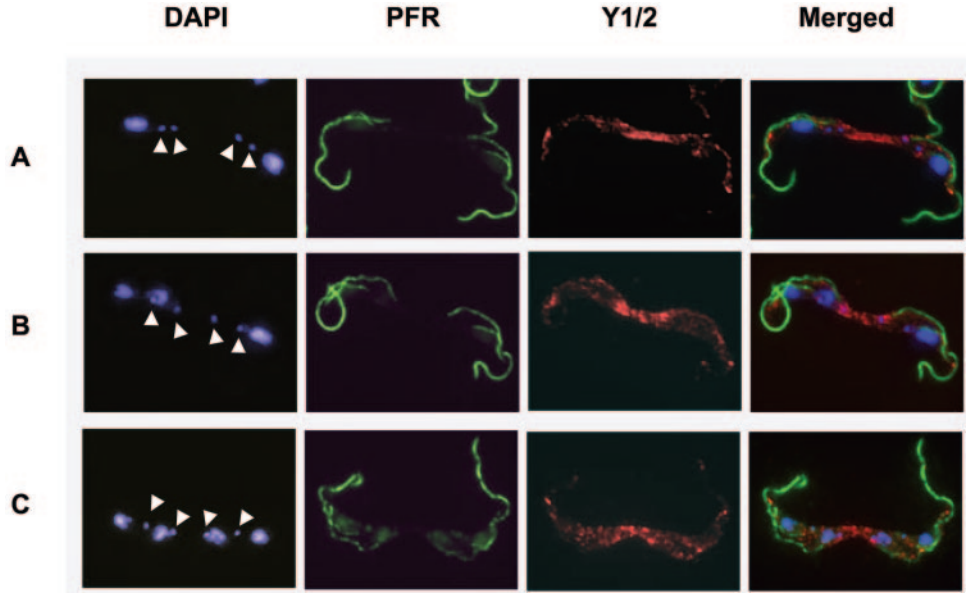

FIG. 3. Morphology of RiD-1 cells defective in the last stages of cytokinesis. The gallery of images shows trypanosomes that had not completed cytokinesis and reinitiated a new cell cycle still being attached at the posterior end ("stuck" phenotype), with four kinetoplasts and two nuclei (A), four kinetoplasts and three nuclei (B), or four kinetoplasts and four nuclei (C). DNA was stained with DAPI, the flagellum was stained with an antibody recognizing the paraflagellar rod, and newly synthesized tubulin was stained with the Y1/2 monoclonal antibody. Arrowheads point to the kinetoplast DNA.

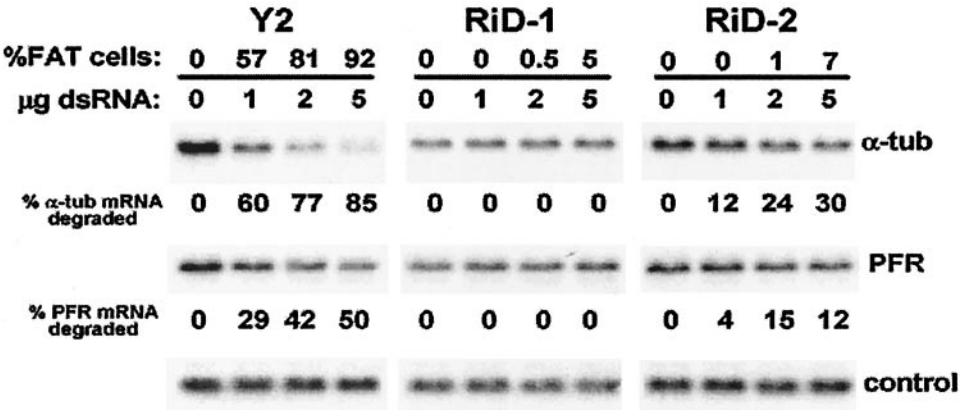

FIG. 4. RNAi-deficient clones RiD-1 and RiD-2 are impaired in degradation of target mRNA. Cells (5×10^7) from the parental wild-type line Y2 or RNA-deficient clones RiD-1 and RiD-2 were simultaneously electroporated with increasing amounts of dsRNA homologous to the 5′ untranslated region of α-tubulin mRNA or to a portion of the coding region of the PFR mRNA. The proportion of FAT cells, indicated above each panel, was determined 16 h after transfection by microscopic observation of live cells. RNA was isolated 2 h after transfection and subjected to Northern blot analysis with probes specific for α-tubulin or PFR mRNA. The bottom panel shows the hybridization to procyclin mRNA, which served as a control for RNA recovery and loading. Hybridization intensities were measured by phosphorimager analysis, and the values were adjusted according to the intensity of the control hybridization. The percentage of mRNA degraded was calculated for each condition by subtracting the amount of mRNA remaining from the amount of input mRNA present in cells that received poly(I:C) as an unspecific dsRNA control (lanes 0).

ability to respond to high concentrations of the dsRNA trigger. Northern analysis confirmed that RiD-1 and RiD-2 trypanosomes are defective in the degradation of target α-tubulin or PFR mRNA (Fig. 4). In particular, RiD-2 cells showed a three- to fivefold decrease in the efficiency of target mRNA degradation. In contrast, the RNAi deficiency of RiD-1 cells was much more pronounced: at the concentrations of dsRNA tested, we could not detect significant degradation of target mRNA in RiD-1 cells. However, at higher dsRNA doses, namely, 10 or 20 μg of dsRNA, a limited amount of target mRNA degradation was also evident in RiD-1 cells (data not shown). From this analysis, we concluded that both RiD-1 and RiD-2 cells were impaired at the effector step of RNAi, namely, degradation of target mRNA.

The observed mRNA degradation defect in RiD-1 and RiD-2 cells could result from inefficient production or accumulation of siRNAs (the initiation step) or could represent a true block at the effector step of the RNAi pathway. To distinguish between these possibilities, we first monitored endogenous siRNAs homologous to the Ingi (Fig. 5A) or SLACS (Fig. 5B) retroposon transcripts by Northern blot hybridization with RNAs derived from Y1, Y2, RiD-1, and RiD-2 cells. This showed that the accumulation of Ingi or SLACS siRNA was not impaired in RiD-1 and RiD-2 cells, compared to their corresponding parent cell lines. Second, we examined whether RiD-1 and RiD-2 cells were defective in the accumulation of siRNAs derived from a transgene. To this end, we generated Y1, Y2, RiD-1, and RiD-2 cell populations constitutively expressing GFP dsRNA as a hairpin RNA (Y1-gfph, Y2-gfph, RiD-1-gfph, and RiD-2-gfph). All four cell lines tested expressed transcripts diagnostic of GFP dsRNA (data not shown). Northern analysis revealed that GFP siRNAs (Fig. 5C) were present in the RNAs derived from RiD-1-gfph (lane 2) and RiD-2-gfph (lane 4) cells in amounts similar to, if not higher than, those present in Y1-gfph (lane 1) and Y2-gfph (lane 3) RNAs. Since the GFP dsRNA-expressing cells represented populations rather than clones, it was possible that the RiD-1 and RiD-2 derivatives had a higher copy number of integrated GFP dsRNA transgenes and that this resulted in larger-than-wild-type amounts of GFP siRNAs. Taken together, the results presented in Fig. 4 and 5 demonstrated that RiD-1 and RiD-2 trypanosomes were wild type with respect to

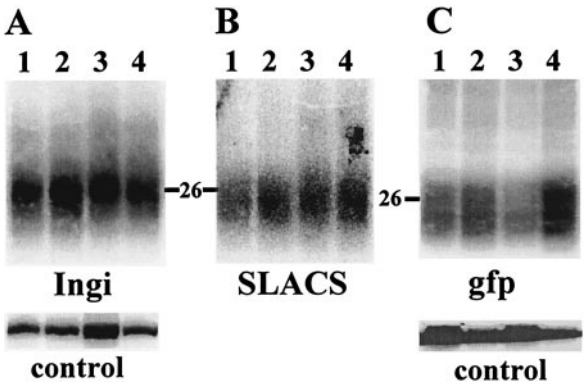

FIG. 5. Accumulation of siRNAs and retroposon-derived transcripts in RNAi-deficient trypanosomes. (A and B) Accumulation of endogenous siRNA homologous to Ingi and SLACS retroposons. Low-molecular-weight RNA from Y1 (lane 1), Y2 (lane 3), RiD-1 (lane 2), or RiD-2 (lane 4) cells was prepared as described previously (6) and electrophoresed on a 15% sequencing gel. After transfer, the filters were hybridized with radiolabeled sense riboprobes as indicated below each panel. (C) Accumulation of siRNAs from a hairpin GFP transgene. For analysis of GFP siRNAs, Y1, Y2, RiD-1, and RiD-2 cells were transformed with a plasmid expressing the coding region of GFP as a hairpin (21) to establish cell populations Y1-gfph (lane 1), Y2-gfph (lane 3), RiD-1-gfph (lane 2), and RiD-2-gfph (lane 4). Small RNAs were analyzed as described above. The panels labeled control show the cross-hybridization to a background band, which served as a control for RNA loading. The migration of a 26-nt DNA marker is indicated by a bar.

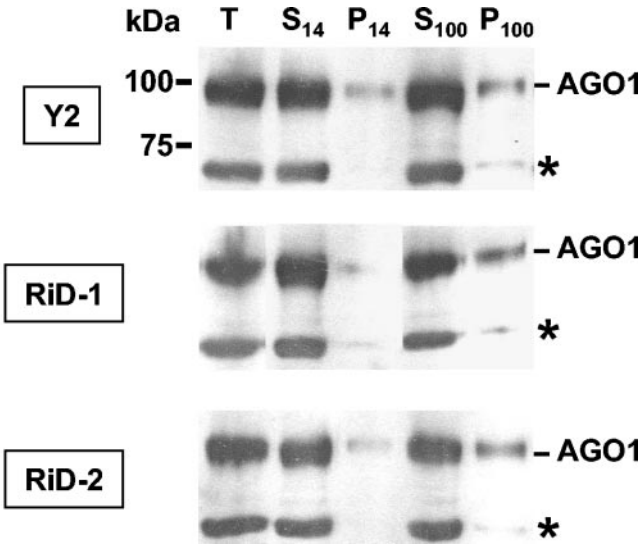

FIG. 6. Expression and fractionation properties of TbAGO1 protein in wild-type and RNAi-deficient cells. Cell extracts were prepared from the various cell lines, as indicated on the left of each panel, and subjected to differential centrifugation as previously described (21). Equivalents aliquots of each subcellular fraction were separated on an SDS–8% polyacrylamide gel, transferred to a nitrocellulose filter, and reacted with a polyclonal rabbit antiserum against TbAGO1 (21). The bound antibody was detected by enhanced chemiluminescence. T, input; S_{14} and P_{14}, supernatant and pellet, respectively, after centrifugation at 14,000 × *g* for 10 min; S_{100} and P_{100}, supernatant and pellet, respectively, after centrifugation at 100,000 × *g* for 60 min. The asterisks indicate a cross-hybridizing band that served as a loading control.

the initiation step but were defective at the effector step of the RNAi pathway.

The sequence or cellular localization of AGO1 is not affected in RiD-1 and RiD-2 trypanosomes. The simplest hypothesis to explain the mRNA cleavage defects of RiD cells was that mutations had been introduced in *TbAGO1*, the putative RNAi endonuclease, resulting in defects in the expression, cellular localization, or catalytic activity of AGO1. Thus, we checked whether the *TbAGO1* gene sequence was mutated in RiD-1 and RiD-2 cells. The *TbAGO1* gene was PCR amplified and sequenced from Y1, Y2, RiD-1, or RiD-2 genomic DNA, but we found no evidence of mutations in the RiD-1 or RiD-2 *AGO1* gene (data not shown). Second, we determined the amount of AGO1 expressed in RiD cells and whether it partitioned between the soluble and polyribosome-bound forms, as is characteristic of AGO1 in wild-type cells. Cell extracts from Y2, RiD-1, and RiD-2 cells were fractionated by differential centrifugation, and the individual fractions were examined by Western blotting with anti-AGO1 polyclonal antibodies (Fig. 6). We did not observe any significant differences among the three cell lines: AGO1 was expressed in RiD-1 and RiD-2 cells in amounts comparable to those present in Y2 cells, and no apparent anomalies in the fractionation behavior of AGO1 could be detected among the three cell extracts. Thus, these experiments excluded the possibility that the mRNA cleavage defects of RiD-1 or RiD-2 cells were due to mutations in the *AGO1* gene or to the failure of AGO1 to associate with polyribosomes.

RiD-1 and RiD-2 trypanosomes accumulate increased amounts of retroposon-derived transcripts. Our previous analysis of AGO1 function in *T. brucei* revealed that genetic ablation of AGO1 resulted in upregulation of retroposon transcripts (21). Thus, we analyzed retroposon transcript abundance in RiD-1 and RiD-2 cells by Northern blotting. Figure 7A shows that, compared to their respective parent Y1 (lane 1) and Y2 (lane 3) cell lines, both RiD-1 (lane 2) and RiD-2 (lane 4) displayed a three- to fivefold increase in the abundance of the heterogenous transcripts homologous to the ubiquitous Ingi retroelement (18). Similar results were obtained for the SLACS transcripts (which are detected as a major band of about 6,000 nt [21]) in RiD-1 (Fig. 7B, compare lanes 1 and 6) or RiD-2 (data not shown) trypanosomes. This analysis showed that RiD cells had the hallmark of RNAi deficiency with respect to the accumulation of retroposon transcripts.

The increase in the steady-state level of retroposon transcripts could be a result of posttranscriptional and/or transcriptional mechanisms. To evaluate this, we chose RiD-1 cells, because they displayed the highest degree of RNAi deficiency. First, we analyzed the decay rate of SLACS transcripts after halting transcription with actinomycin D (Fig. 7B and C). In contrast, Ingi transcripts do not lend themselves to this analysis because they are too heterogeneous in size. The results showed that the half-life of SLACS transcripts in RiD-1 cells was approximately doubled compared to that in wild-type cells (Fig. 7C). Next, we quantitated the transcription of both SLACS and Ingi retroelements by hybridizing radiolabeled RNA synthesized in permeable cells to gene-specific fragments immobilized on a membrane (Fig. 7D). As controls for this experiment, we used RNAs derived from wild-type as well as from *ago1*$^{-/-}$ cells. Relative to that in the wild-type control, transcription of Ingi and SLACS retroelements was increased in RiD-1 cells, and the magnitude of the increase was similar to that observed in *ago1*$^{-/-}$ cells.

DISCUSSION

Here we have exploited the ability of α-tubulin dsRNA to block cytokinesis in wild-type cells to enrich for trypanosomes that were unable to respond to this challenge. We assumed that among the α-tubulin dsRNA-resistant cells, we might be able to identify trypanosomes defective in the RNAi pathway. The selection scheme was indeed successful and resulted in the isolation of RNAi-deficient trypanosomes that survived challenge with α-tubulin dsRNA, because they were severely impaired in executing degradation of α-tubulin mRNA.

The enrichment for α-tubulin dsRNA-resistant cells occurred stepwise, and it was only after five cycles of selection that we routinely obtained populations in which more than 90% of the cells were no longer responding to α-tubulin dsRNA. This was observed irrespective of whether uncloned or freshly cloned trypanosomes of our procyclic laboratory strain were used as starting populations. In contrast, when we applied the same selection procedure to two other trypanosome strains of independent origin, we found that seven to eight selection cycles were required to obtain relatively homogeneous populations resistant to challenge with α-tubulin dsRNA. This indicated that there are strain differences with respect to the recovery of RNAi-deficient cells by our selection procedure.

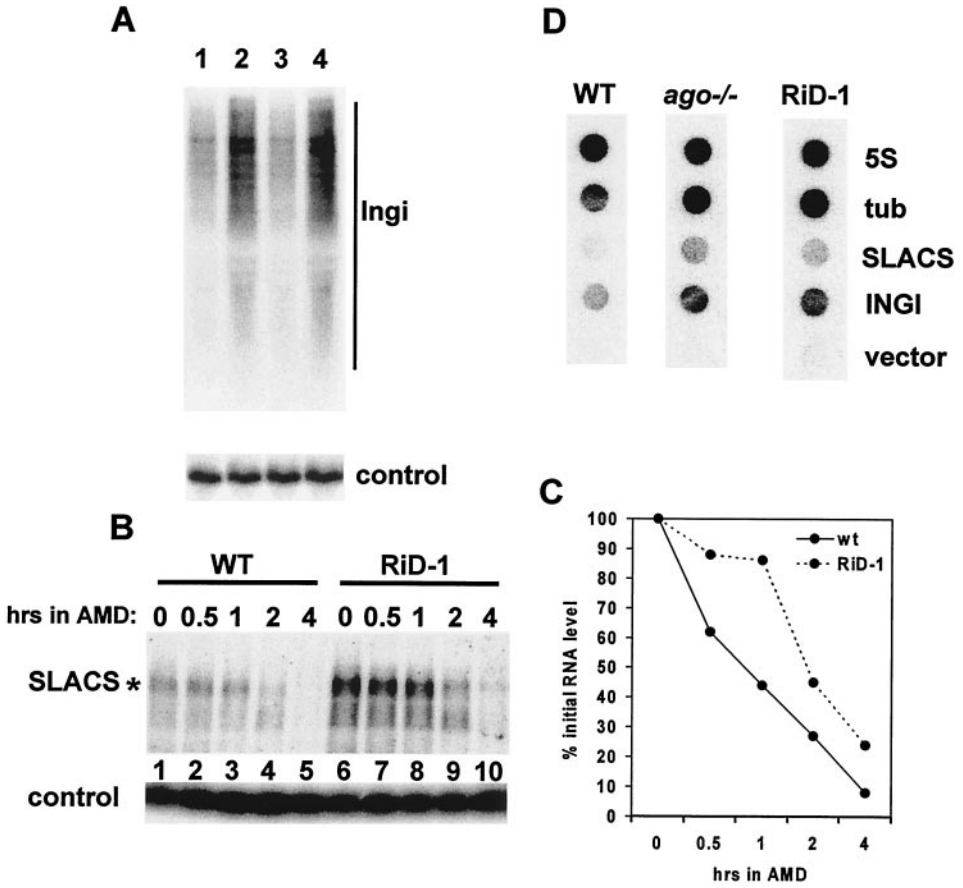

FIG. 7. Analysis of retroposon transcripts in RiD cells. (A) The level of Ingi retroposon transcripts is increased in RNAi-deficient trypanosomes. Total RNA from Y1 (lane 1), Y2 (lane 3), RiD-1 (lane 2), or RiD-2 (lane 4) was fractionated on a 1.2% agarose-formaldehyde gel and analyzed by Northern blotting with a radiolabeled DNA probe representing a portion of the Ingi retroelement. The filter was stripped and hybridized to a α-tubulin probe to control for RNA loading (control panel). (B) Northern blot of SLACS transcripts in wild-type and RiD-1 cells over a period of 4 h following the addition of 10 μg of actinomycin D (AMD) per ml. The prominent, approximately 6,000-nt-long SLACS transcripts are indicated by an asterisk. The identities of the smaller transcripts below the major band are unknown, and these bands are not consistently detected. Hybridization to 5S RNA served as a loading control (control panel). WT, wild type. (C) Quantitation of the hybridization results shown in panel B. Hybridization intensities of the 6,000-nt SLACS transcripts were measured by phosphorimager analysis, and the values were adjusted according to the intensity of the control hybridization. Data are plotted as percentages of the RNA present at time zero. (D) Radiolabeled RNA synthesized in permeable wild-type, *ago1*$^{-/-}$, or RiD-1 cells was hybridized to the following DNAs spotted onto a nitrocellulose filter: 5S rRNA (5S), α-tubulin (tub), SLACS, Ingi, and plasmid vector (vector).

The higher rate of acquisition of RNAi deficiency in our laboratory strain might be due to heterozygosity at one or more loci that carry genes that are directly or indirectly involved in the RNAi pathway.

The RiD-1 and RiD-2 clones were chosen for detailed analysis, because they were derived from independent selections with α-tubulin dsRNA and because they showed the highest degree of resistance to challenge with α-tubulin dsRNA, as initially measured by their deficiency in acquiring the FAT phenotype. Nevertheless, analysis of 30 clonal lines, derived from α-tubulin dsRNA-resistant Y1 and Y2 cell populations, revealed heterogeneity among the clones in the degree of resistance to α-tubulin dsRNA. Cumulatively, about 25% of the clones displayed between 1 and 2% FAT cells, about 50% gave rise to between 5 and 10% FAT cells, and the remaining clones displayed more than 10% FAT cells (data not shown). These observations are consistent with the possibility that acquisition of resistance to α-tubulin dsRNA occurred independently in several cells of the Y1 or Y2 starting cell population. However, since we did not identify the genes responsible for the RiD-1 or RiD-2 phenotype, it is unclear whether RiD-1 and RiD-2 might be allelic.

In principle, identification of the genetic lesion(s) in RiD-1 and RiD-2 trypanosomes could be achieved by genetic complementation. Genetic complementation was reported several years ago for one mutant *T. brucei* strain, namely, a null mutant for the ornithine decarboxylase gene (22). To attempt complementation of RiD clones, we generated RiD-1 and RiD-2 reporter strains expressing GFP and GFP dsRNA. We reasoned that upon transfection with a genomic library, we might be able to select for cells that had lost GFP fluorescence, because the function of the RNAi pathway had been restored. However, after a few weeks in culture the reporter strains accumulated a considerable number of cells that no longer expressed GFP. This indicated that in some cells the GFP gene had been "naturally" silenced, thus negating the possibility for complementation.

At the cellular level, RiD-1 and RiD-2 cells displayed different growth characteristics. Both the doubling time and the cell cycle status of RiD-2 cells were similar, but not identical, to those of wild-type cells. In contrast, RiD-1 cells showed approximately a 30% delay in cell division, as well as accumulation of "stuck" cells that were unable to terminate cytokinesis. Intriguingly, these abnormalities closely paralleled those of the *ago1*$^{-/-}$ cells that we previously established in our laboratory strain. However, the small proportion of stuck cells that we detected in RiD-1 and *ago1*$^{-/-}$ trypanosomes does not seem sufficient to account for the observed 30% increase in the duration of the cell cycle. It is likely that the number of cells with defects at terminating cytokinesis might have been underestimated in our analysis, because the stuck phenotype could be identified with certainty only if cells had reentered the cell cycle. Defects in the last stages of cytokinesis in *S. pombe* mutants lacking the *dicer1* or *ago1* gene have been recently reported (2). In this case it was shown that *ago1* or *dicer1* is required for regulated hyperphosphorylation of Cdc2 kinase when encountering genotoxic insults and that this results in abnormal cytokinesis, cell cycle arrest deficiencies, and mating defects. In contrast, in *T. brucei* there seems to be no nuclear mitosis/cytokinesis checkpoint in that cytokinesis can proceed in the absence of mitosis (20) and, conversely, kinetoplast segregation and mitosis can occur in the absence of cytokinesis (19). These observations point to fundamental differences between trypanosomes and other eukaryotes in terms of cell cycle control. Clearly, understanding of how RNAi deficiency affects the cell cycle of *T. brucei* requires further investigation. Lastly, it should be noted that the growth defects we observe in the RNAi-deficient cells established in our trypanosome laboratory strain are far less dramatic than those reported for an *AGO1* null cell line derived from *T. brucei* 427 procyclics (7). One possibility to reconcile these different results is that the severity of the cellular consequences which are observed upon eliminating or downregulating the RNAi pathway is influenced by the genetic backgrounds of the different trypanosome strains used for the experiments. It is also possible, as we discussed previously (25), that the cellular defects observed upon elimination of the RNAi pathway may result, at least in part, from the accumulation of mutations due to the potential mobilization of retroposons in RNAi-deficient cells. We have recently constructed a strain in which the AGO1 gene is conditionally expressed. Thus, it should now be possible to assess the timing of appearance and extent of cellular defects when RNAi is downregulated and to distinguish between direct and indirect effects of RNAi deficiency.

Both RiD-1 and RiD-2 trypanosomes turned out to be deficient in the RNAi pathway, although the RNAi deficiency was not absolute, as these cells retain a limited capacity to carry out degradation of target mRNAs at high concentrations of trigger dsRNA. One possible explanation of this phenomenon is that at high concentrations of trigger dsRNA there should be a greater proportion of AGO1 loaded with the specific siRNAs, and this might bypass to some extent the defect(s) in RiD cells. The observation that both RiD clones were severely impaired in degradation of two different target mRNAs indicated that the RNAi deficiency was not restricted to α-tubulin mRNA. Since accumulation of endogenous retroposon-derived or transgene-derived siRNAs was not affected, we concluded that the effector step of RNAi, namely, degradation of target mRNA, was impaired. However, the RNAi-deficient phenotype of RiD-1 and RiD-2 cells was not a consequence of mutations in the *AGO1* gene or of defects in the expression level or cellular distribution of the AGO1 protein. Taken together, our results indicated that neither the processing of dsRNA nor AGO1 was altered in RiD trypanosomes. Rather, the phenotypes of RiD cells point to a step affecting the efficiency of cleavage of mRNA by AGO1. It is possible that the RiD genetic lesion(s) affects the function of one or more components required to interact with AGO1 to bring about efficient cleavage of mRNA. In this scenario, in vivo the endonuclease activity of AGO1 might be regulated by interaction with this putative factor(s). A second possibility is that the activity of AGO1 might be regulated by posttranslational modifications, such as phosphorylation or methylation, which are also known to modify protein-protein interactions. We have recently found that AGO1 is posttranslationally methylated at arginine residues in the amino-terminal RGG domain (N. Chamond et al., unpublished observation), thus supporting the hypothesis that AGO1 function might be modulated by methylation. Once the function of these modified arginine residues is understood, it will be interesting to determine whether AGO1 in RiD cells is appropriately modified.

Both RiD clones had a pronounced increase in the steady-state level of retroposon transcripts, the hallmark of genetic ablation of the RNAi pathway in trypanosomes. Similar to the case for *ago1*$^{-/-}$ cells (21), the increased steady-state level of SLACS retroposon transcripts in RiD-1 cells was brought about by an increase in the stability of the retroposon transcripts and in the transcription of the corresponding retroelements. However, it should be pointed out that the increase in stability of SLACS transcripts in RiD-1 cells was not as pronounced as that in *ago1*$^{-/-}$ cells, namely, a twofold increase in RiD-1 cells versus a fourfold increase in *ago1*$^{-/-}$ cells (21). This difference could be explained by the fact that RiD-1 cells still retain some ability to cleave mRNA, whereas *ago1*$^{-/-}$ cells are functionally RNAi negative.

The observation that RiD-1 trypanosomes display an increased transcription of retroelements, which is similar to that of *ago1*$^{-/-}$ cells, further supports the possibility that the RNAi pathway has a role, either direct or indirect, in regulating transcription of retroelements. By analogy to the function of the RNAi pathway in heterochromatin formation in *S. pombe* (27), it is plausible that in *T. brucei* the absence of a functional RNAi pathway results in changes in chromatin structure leading to an increased accessibility of retroelements to the RNA polymerase II transcriptional machinery. On the other hand, one could imagine that the retroposon transcripts themselves or perhaps the proteins encoded by retroposon mRNAs might have a role in regulating transcription of the elements in the genome.

ACKNOWLEDGMENTS

This work was supported by NIH grants AI28798 and AI056333 to E.U.

REFERENCES

1. **Bastin, P., K. Ellis, L. Kohl, and K. Gull.** 2000. Flagellum ontogeny in trypanosomes studied via an inherited and regulated RNA interference system. J. Cell Sci. **113:**3321–3328.

2. **Carmichael, J. B., P. Provost, K. Ekwall, and T. C. Hobman.** 2004. ago1 and dcr1, two core components of the RNA interference pathway, functionally diverge from rdp1 in regulating cell cycle events in *Schizosaccharomyces pombe*. Mol. Biol. Cell **15:**1425–1435.
3. **Caudy, A. A., R. F. Ketting, S. M. Hammond, A. M. Denli, A. M. Bathoorn, B. B. Tops, J. M. Silva, M. M. Myers, G. J. Hannon, and R. H. Plasterk.** 2003. A micrococcal nuclease homologue in RNAi effector complexes. Nature **425:**411–414.
4. **Caudy, A. A., M. Myers, G. J. Hannon, and S. M. Hammond.** 2002. Fragile X-related protein and VIG associate with the RNA interference machinery. Genes Dev. **16:**2491–2496.
5. **Djikeng, A., H. Shi, C. Tschudi, S. Shen, and E. Ullu.** 2003. An siRNA ribonucleoprotein is found associated with polyribosomes in *Trypanosoma brucei*. RNA **9:**802–808.
6. **Djikeng, A., H. Shi, C. Tschudi, and E. Ullu.** 2001. RNA interference in *Trypanosoma brucei*: cloning of small interfering RNAs provides evidence for retroposon-derived 24–26-nucleotide RNAs. RNA **7:**1522–1530.
7. **Durand-Dubief, M., and P. Bastin.** 2003. TbAGO1, an Argonaute protein required for RNA interference is involved in mitosis and chromosome segregation in *Trypanosoma brucei*. BMC Biol. **1:**2. [Online.] http://www.biomedcentral.com.
8. **Hall, I. M., K. Noma, and S. I. Grewal.** 2003. RNA interference machinery regulates chromosome dynamics during mitosis and meiosis in fission yeast. Proc. Natl. Acad. Sci. USA **100:**193–198.
9. **Hall, I. M., G. D. Shankaranarayana, K. Noma, N. Ayoub, A. Cohen, and S. I. Grewal.** 2002. Establishment and maintenance of a heterochromatin domain. Science **297:**2232–2237.
10. **Hannon, G. J.** 2002. RNA interference. Nature **418:**244–251.
11. **Ishizuka, A., M. C. Siomi, and H. Siomi.** 2002. A Drosophila fragile X protein interacts with components of RNAi and ribosomal proteins. Genes Dev. **16:**2497–2508.
12. **Lau, N. C., L. P. Lim, E. G. Weinstein, and D. P. Bartel.** 2001. An abundant class of tiny RNAs with probable regulatory roles in *Caenorhabditis elegans*. Science **294:**858–862.
13. **Lee, R. C., and V. Ambros.** 2001. An extensive class of small RNAs in *Caenorhabditis elegans*. Science **294:**862–864.
14. **Liu, J., M. A. Carmell, F. V. Rivas, C. G. Marsden, J. M. Thomson, J. J. Song, S. M. Hammond, L. Joshua-Tor, and G. J. Hannon.** 2004. Argonaute2 is the catalytic engine of mammalian RNAi. Science [Online.] http://www.sciencemag.org.
15. **Liu, Q., T. A. Rand, S. Kalidas, F. Du, H. E. Kim, D. P. Smith, and X. Wang.** 2003. R2D2, a bridge between the initiation and effector steps of the Drosophila RNAi pathway. Science **301:**1921–1925.
16. **Mette, M. F., W. Aufsatz, J. van Der Winden, M. A. Matzke, and A. J. Matzke.** 2000. Transcriptional silencing and promoter methylation triggered by double-stranded RNA. EMBO J. **19:**5194–5201.
17. **Mochizuki, K., N. A. Fine, T. Fujisawa, and M. A. Gorovsky.** 2002. Analysis of a piwi-related gene implicates small RNAs in genome rearrangement in tetrahymena. Cell **110:**689–699.
18. **Murphy, N. B., A. Pays, P. Tebabi, H. Coquelet, M. Guyaux, M. Steinert, and E. Pays.** 1987. *Trypanosoma brucei* repeated element with unusual structural and transcriptional properties. J. Mol. Biol. **195:**855–871.
19. **Ngo, H., C. Tschudi, K. Gull, and E. Ullu.** 1998. Double-stranded RNA induces mRNA degradation in *Trypanosoma brucei*. Proc. Natl. Acad. Sci. USA **95:**14687–14692.
20. **Robinson, D. R., T. Sherwin, A. Ploubidou, E. H. Byard, and K. Gull.** 1995. Microtubule polarity and dynamics in the control of organelle positioning, segregation, and cytokinesis in the trypanosome cell cycle. J. Cell Biol. **128:**1163–1172.
21. **Shi, H., A. Djikeng, C. Tschudi, and E. Ullu.** 2004. Argonaute protein in the early divergent eukaryote *Trypanosoma brucei*: control of small interfering RNA accumulation and retroposon transcript abundance. Mol. Cell. Biol. **24:**420–427.

21a. **Shi, H., C. Tschudi, and E. Ullu.** 21 September 2004. Function of the trypanosome argonaute 1 protein in RNA interference requires the N-terminal RGG domain and arginine 735 in the piwi domain. J. Biol. Chem. 10.1074/jbc.M409280200.

22. **Sommer, J. M., S. Hua, F. Li, K. M. Gottesdiener, and C. C. Wang.** 1996. Cloning by functional complementation in *Trypanosoma brucei*. Mol. Biochem. Parasitol. **76:**83–89.
23. **Tomari, Y., T. Du, B. Haley, D. S. Schwarz, R. Bennett, H. A. Cook, B. S. Koppetsch, W. E. Theurkauf, and P. D. Zamore.** 2004. RISC assembly defects in the Drosophila RNAi mutant armitage. Cell **116:**831–841.
24. **Ullu, E., and C. Tschudi.** 1990. Permeable trypanosome cells as a model system for transcription and trans-splicing. Nucleic Acids Res. **18:**3319–3326.
25. **Ullu, E., C. Tschudi, and T. Chakraborty.** 2004. RNA interference in protozoan parasites. Cell. Microbiol. **6:**509–519.
26. **van Deursen, F. J., S. K. Shahi, C. M. Turner, C. Hartmann, C. Guerra-Giraldez, K. R. Matthews, and C. E. Clayton.** 2001. Characterisation of the growth and differentiation in vivo and in vitro of bloodstream-form *Trypanosoma brucei* strain TREU 927. Mol. Biochem. Parasitol. **112:**163–171.
27. **Verdel, A., S. Jia, S. Gerber, T. Sugiyama, S. Gygi, S. I. Grewal, and D. Moazed.** 2004. RNAi-mediated targeting of heterochromatin by the RITS complex. Science **303:**672–676.
28. **Volpe, T., V. Schramke, G. L. Hamilton, S. A. White, G. Teng, R. A. Martienssen, and R. C. Allshire.** 2003. RNA interference is required for normal centromere function in fission yeast. Chromosome Res. **11:**137–146.
29. **Volpe, T. A., C. Kidner, I. M. Hall, G. Teng, S. I. Grewal, and R. A. Martienssen.** 2002. Regulation of heterochromatic silencing and histone H3 lysine-9 methylation by RNAi. Science **297:**1833–1837.
30. **Wang, Z., and P. T. Englund.** 2001. RNA interference of a trypanosome topoisomerase II causes progressive loss of mitochondrial DNA. EMBO J. **20:**4674–4683.
31. **Wirtz, E., S. Leal, C. Ochatt, and G. A. Cross.** 1999. A tightly regulated inducible expression system for conditional gene knock-outs and dominant-negative genetics in Trypanosoma brucei. Mol. Biochem. Parasitol. **99:**89–101.
32. **Zilberman, D., X. Cao, and S. E. Jacobsen.** 2003. ARGONAUTE4 control of locus-specific siRNA accumulation and DNA and histone methylation. Science **299:**716–719.